RSC Advances

PAPER

View Article Online
View Journal | View Issue

Cite this: *RSC Adv.*, 2016, **6**, 56668

Probing the structural and magnetic properties of a new family of centrosymmetric dinuclear lanthanide complexes†

Y. Jiang,[a] R. J. Holmberg,[a] F. Habib,[a] L. Ungur,‡[b] I. Korobkov,[a] L. F. Chibotaru[b] and M. Murugesu*[a]

Received 9th May 2016
Accepted 7th June 2016

DOI: 10.1039/c6ra12070a

www.rsc.org/advances

A series of centrosymmetric dinuclear lanthanide complexes, including Gd^{III} (**1**), Dy^{III} (**2**), Ho^{III} (**3**), Er^{III} (**4**) and Yb^{III} (**5**), have been synthesized and studied for the effects of lanthanide contraction on their magnetic properties. As a result of probing the magnetic properties of the Gd^{III} analogue, **1**, a weak antiferromagnetic intramolecular interaction was confirmed, with $J = -0.01$ cm^{-1} and $g = 2.01$. The Dy^{III} complex, **2**, was found to exhibit larger values of g_x and g_y in the ground doublet of individual Dy^{III} ions *via ab initio* calculations, and thus did not act as a SMM. Interestingly, the Er^{III} (**4**) and Yb^{III} (**5**) complexes exhibited slow relaxation of the magnetization under an applied dc field with effective energy barriers (U_{eff}) of 21 K and 22 K, respectively.

Introduction

The emergence of lanthanide Single-Molecule Magnets (SMMs) in the past decade has significantly revamped the area of molecular nanomagnetism.[1–4] This is primarily due to the development of SMMs with the significant inherent magnetic anisotropy of lanthanide ions. Despite the extensive work performed on lanthanide complexes, there are very few reports of early lanthanide metal ions exhibiting SMM behaviour,[5–9] thus, this research field is primarily dominated by late, heavier lanthanide ions as they possess significantly larger spin–orbit coupling constants (ζ), as well as larger total electronic angular momentum quantum number (J) values. Currently, the best performing SMMs have been isolated with late lanthanide metals such as Dy^{III}, Tb^{III} and Er^{III} ions.[10–14] Mononuclear lanthanide SMMs are ideal model systems as they provide unique insights into the factors that influence spin–orbit coupling constants and ground spin multiplets. Therefore, these systems have been developed over the last decade to provide experimentally powerful answers to those who continue their quest toward high-energy barrier SMMs. Recently, exciting results have been attained through fine-tuning the crystal field around the metal centre to achieve record breaking blocking temperatures for mononuclear SMMs,[10,12–14] furthermore even greater barriers have been theoretically predicted for such systems.[15–17] That being said, one major limiting factor is important to consider if we want SMMs to advance towards being operational at room temperature; mononuclear SMMs are limited to one single metal centre, which implies that, at the end of the day, the anisotropy and/or the total spin will be quantitatively limited. Therefore, polynuclear SMMs are likely the future of this field.

In order to efficiently construct multimetallic lanthanide SMMs, it is critical to gain design control over the interactions between metal ions. This is a continuous challenge, especially since the interactions between lanthanide ions are almost negligible in strength owing to their core 4f orbitals. Thus, dinuclear systems, in particular, are ideal models to probe interactions between metal ions, as well as the influence of structural changes on the overall magnetic behaviour of SMMs. This is especially true since dinuclear SMMs have been shown to possess the capability to be incredibly high performing magnets.[10,18–25]

With this in mind we have focused our attention on studying a new system; a family of centrosymmetric complexes isolated using a highly tuneable Schiff base system, which was based on an *o*-Vanillin moiety. We have previously demonstrated this strategy to be highly efficient towards isolating dinuclear complexes with non-negligible energy barriers. As an extension to our previous work, we have targeted the synthesis and use of (*E*)-2-(dimethylamino)-*N*′-(2-hydroxy-3-

[a]*Department of Chemistry and Biomolecular Sciences, University of Ottawa, 10 Marie Curie, Ottawa, ON, Canada K1N 6N5. E-mail: m.murugesu@uottawa.ca; Tel: +1 613 562 5800 ext. 2733*

[b]*Theory of Nanomaterials Group and INPAC Institute for Nanoscale Physics and Chemistry, Katholieke Universiteit Leuven, Celestijnenlaan, 200F, 3001 Leuven, Belgium*

† Electronic supplementary information (ESI) available: Crystallographic information, PXRD, SQUID magnetic measurements, details of DFT calculations, and supplementary figures. CCDC 1426599–1426602. For ESI and crystallographic data in CIF or other electronic format see DOI: 10.1039/c6ra12070a

‡ Temporary address: Theoretical Chemistry, Lund University, Getingevagen 60, 22241, Lund, Sweden.

methoxybenzylidene) acetohydrazide (H_2ovgrd) (Chart 1) as a new ligand for the isolation of dinuclear lanthanide systems.

As aforementioned, we directed our efforts toward the isolation of molecules with heavier lanthanide ions (Ln^{III} = Gd, Dy, Ho, Er and Yb) in order to probe the SMM properties, while also investigating the effects of lanthanide contraction and its influence on the structural changes. Herein, we report a family of centrosymmetric complexes synthesized using H_2ovgrd and Ln^{III} ions with emphasis on the study of their structural, physical, and specifically their unique magnetic properties.

Experimental

Materials and methods

All chemicals were of reagent grade, purchased from TCI, Alfa Aesar, and Strem Chemicals and were used without any further purification.

Synthesis

(*E*)-2-(Dimethylamino)-*N*′-(2-hydroxy-3-methoxybenzylidene) acetohydrazide (H_2ovgrd). The employed ligand (Chart 1) was synthesized by adding Girard's reagent D (380.12 mg, 2 mmol) and pyridine (314.4 mg, 4 mmol) into 20 mL of MeOH, and stirring the mixture until complete dissolution was achieved. *O*-Vanillin (304.3 mg, 2 mmol) in 5 mL MeOH was added to the previous solution and treated with stirring for 2 hours at room temperature. The resulting pale yellow coloured product was collected and washed with cold MeOH. Yield = 68%. Calc. (found): C, 12.01 (12.30); H, 1.01 (0.95); N, 14.01 (13.83); O, 16.00 (16.17); ^{1}H NMR (MeOD, 400 MHz): δ 8.39 (s, 1H), 7.24 (d, 1H), 6.99 (d, 1H), 6.83 (t, 1H), 4.52 (s, 2H), 4.10 (s, 1H), 3.88 (s, 3H), 3.00 (s, 6H). Selected IR (cm^{-1}): 3367 (br), 2900 (w), 2627 (br), 1474 (s), 1409 (w), 1374 (m), 1276 (s), 1259 (m), 1241 (m), 1205 (w), 1149 (s), 1255 (s), 1226 (m), 1203 (w), 1184 (w), 1145 (w), 1052 (s), 1009 (m), 975 (m), 965 (m), 912 (w), 859 (w), 764 (s), 725 (s), 610 (m).

$[Ln^{III}_2(ovgrd)_2(acac)_2(H_2O)_2]\cdot 2EtOH$, where Ln = Gd (1), Dy (2), Ho (3), Er (4) and Yb (5). H_2ovgrd (50.26 mg, 0.2 mmol) in 10 mL MeCN was treated with tetraethylammonium hydroxide (TEAOH, 264 μL, 0.4 mmol), and a solution of corresponding $Ln(acac)_3\cdot 6H_2O$ (0.2 mmol) in 5 mL EtOH was subsequently added. The mixture was stirred for 2 min, then filtered. Light yellow to pale pink coloured needle-like crystals were isolated within the range of a few hours to 3 days in ~40–60% yield. All complexes exhibit similar IR spectra therefore selected IR peaks for the Dy analogue are given below as an example. Selected IR (cm^{-1}) for **2**: 3242 (br), 2965 (w), 2832 (w), 1402 (s), 1360 (s), 1309 (s), 1238 (s), 1184 (m), 1129 (m), 1106 (s), 1263 (w), 1233 (m), 1211 (s), 1102 (w), 1080 (w), 1049 (w), 1020 (m), 988 (w), 950 (s), 923 (m), 855 (s), 769 (m), 734 (s).

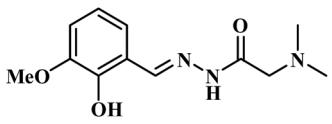

Chart 1 The Schiff base ligand H_2ovgrd.

Characterization

X-ray crystallography. For complexes **1–5**, single crystals suitable for X-ray diffraction measurements were mounted on a glass fibre. Unit cell measurements and intensity data collections were performed on a Bruker-AXS SMART 1 k CCD diffractometer using graphite monochromated MoKα radiation (λ = 0.71073 Å). The data reduction included a correction for Lorentz and polarization effects, with an applied multi-scan absorption correction (SADABS). The crystal structure was solved and refined using the SHELXTL program suite. Direct methods yielded all non-hydrogen atoms, which were refined with anisotropic thermal parameters. All hydrogen atom positions were calculated geometrically and were riding on their respective atoms.

Magnetic measurements. The magnetic susceptibility measurements were obtained using a Quantum Design SQUID magnetometer MPMS-XL7 in the temperature range of 1.8–300 K for dc-applied fields ranging from −7 to 7 T. Dc analyses were performed on polycrystalline samples of 7.8, 7.7, 19.5, 11.9, 7.8 mg for **1–5**, respectively. All samples were wrapped in a polyethylene wrap and measured under a field ranging from 0 to 7 T in the temperature range of 1.8–300 K. Ac susceptibility measurements were carried out under an oscillating ac field of 3 Oe and at frequencies ranging from 0.1 to 1500 Hz. The magnetization data was initially collected at 100 K in order to check for potential ferromagnetic impurities, found to be absent in all samples. A diamagnetic correction was applied for the sample holder and any grease employed to restrain microcrystals, thus preventing torqueing under high fields.

Infrared spectrometry. IR spectra were collected on all samples in the solid state on a Varian 640 FT-IR spectrometer in the 525–4000 cm^{-1} range.

X-ray powder diffraction. X-ray powder diffraction data for complex **5** was collected using RIGAKU Ultima IV, with Cu-Kα radiation (λ = 1.541836 Å), and a graphite monochromator. Scanning of the 2θ range from 5 to 40° was performed. The structure of the sample was confirmed by comparison between the collected pattern and the simulated pattern from the single crystal XRD data of each complex.

NMR. NMR analyses were conducted on a Bruker Avance 400 MHz spectrometer equipped with an automatic sample holder and a 5 mm auto tuning broadband probe with Z gradient.

Results and discussion

Structural analysis

The single crystal X-ray crystallography studies reveal that complexes **1–3** are isostructural, and crystallize in either the monoclinic $P2_1/n$ or $P2_1/c$ space group. The analogous compound with Er^{III}, **4**, shows a slightly different structural arrangement, specifically, its space group is $P\bar{1}$ (Table S1†), and with PXRD measurements it was confirmed that the structure of complex **5**, with Yb^{III}, is in good agreement with that of complex

4 (Fig. S1†). Since the structures of each analogous complex are indeed so similar, this allows us to take the Dy^{III} analogue, **2**, as an example herein (Fig. 1), in order to describe these structures fully. The dinuclear complex contains two eight-coordinate Dy^{III} ions bridged by alkoxide groups (O3, O3a) from two antiparallel doubly-deprotonated ovgrd ligands, forming a centrosymmetric complex. The Dy1···Dy1a distance is 3.98 Å and the Dy1–O3–Dy1a angle is equal to 113.63° (Table S2†). In addition to the bridging alkoxide groups, the coordination sphere around Dy^{III} ions is composed of nitrogen atoms form the tertiary amine (N3), hydrazide nitrogen (N1) and a phenoxide oxygen (O1) from the ovgrd ligand. The remainder of the coordination environment is occupied by one acetylacetone group (O4, O5) and one water molecule (O6), binding on each side. Thus each Dy^{III} exhibits an overall N_2O_6 coordination environment with distorted dodecahedral geometry (Fig. 1). The coordinated water molecules (O6) participate in intramolecular hydrogen bonding with the phenoxide and acac groups, as well as with non-coordinated EtOH, thus keeping the molecule structurally compact. Through careful inspection of the packing arrangement (Fig. S2†), the shortest intermolecular Dy···Dy distance is found to be 8.39 Å.

Lanthanide contraction study

Lanthanide chemistry generally affords structurally analogous complexes as a result of their common chemical attributes. However, in a lanthanide series there exist finite changes in the structure that can be seen due to lanthanide contraction. In some cases full structural rearrangements can be observed.[26] This could subsequently affect the overall physical properties of the molecule. In order to investigate such structural changes, lanthanide contraction studies were performed. The average Ln–X (X = O, N) distances for complexes **1–4** were found to be 2.59, 2.56, 2.55 and 2.54 Å, respectively. These values were then used to extract the shielding constants of the 4f electrons.[27] As expected, they follow the trend of lanthanide contraction, that is, with increasing atomic number n, the average distance decreases. From previous reports, the decay of bond lengths with this contraction follows a quadratic function corresponding to the number, n, of f electrons.[28] Based on our systems, the centrosymmetry allows us to simply study the Ln–X distances by taking the average value of Ln–O and Ln–N bond distances. The best-fit parameters were found to be: $a = 2.6429$, $b = -0.0038$ and $c = -0.0005$ with $R^2 = 0.9946$, which were employed within the quadratic function $F(n) = a + bn + cn^2$ (Fig. 3).

The $d_{(O\cdots O)}$, which represents the distance between oxygen atoms (O3···O3a) that are shared by the coordination polyhedra, was also analysed (Fig. 2). Consequently, it also results in a quadratic decay, with the best-fit parameters of $a = 2.7148$, $b = -0.0061$ and $c = -0.0007$, with $R^2 = 0.9923$. Such an observation could be attributed to the manifestation of lanthanide contraction on parameters affected by two lanthanide atoms simultaneously.[29] This result necessitated further corroboration by plotting the dependence of Ln1···Ln1a distances on n, which exhibits similar behaviour. The quadratic function parameters for $d_{(Ln\cdots Ln)}$ are: $a = 3.8793$, $b = 0.0414$ and $c = -0.0034$ with $R^2 = 0.9921$.

Magnetic properties

In order to correlate the lanthanide contraction study and coordination environment change with the magnetic properties of all complexes, direct current (dc) and alternating current (ac) magnetic susceptibility measurements were performed on crushed polycrystalline samples. The observed room temperature χT value for **1** of 15.84 cm^3 K mol^{-1} is in good agreement with the expected spin only value for two uncoupled Gd^{III} ions ($^8S_{7/2}$, $S = 7/2$, $\chi T = 15.76$ cm^3 K mol^{-1}). Upon decreasing the temperature, the χT product remains constant ~20 K before decreasing rapidly at lower temperatures (Fig. 3). Such behaviour is indicative of dominant antiferromagnetic interactions between the metal centres. Moreover, thanks to the isotropic nature of Gd^{III} ions, by applying the Van Vleck equation to Kambe's vector coupling scheme, the magnetic interaction between the two spin centers could be quantified, and was calculated to be $J = -0.01$ cm^{-1} with $g = 2.01$. This interaction is rather weak, as is expected for a dinuclear system with 4f ions.[26] The field dependence of the magnetization at low temperatures

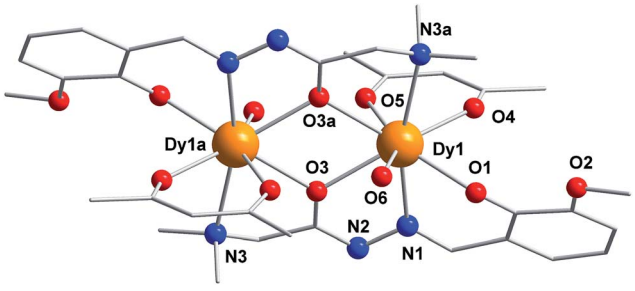

Fig. 1 Partially labelled molecular structure of centrosymmetric dinuclear complex $[Dy^{III}_2(ovgrd)_2(acac)_2(H_2O)_2]$, **2**, hydrogen atoms and solvent molecules have been omitted for clarity. Colour code: orange (Dy), red (O), blue (N) and grey (C).

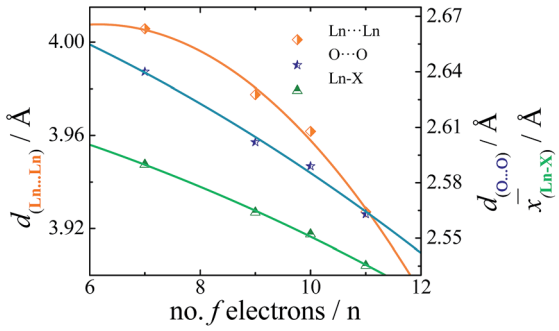

Fig. 2 Graph of Ln···Ln distances, O···O distances and average Ln–X (X = O, N) bond lengths *versus* the number of 4f electrons (n) for complexes **1** to **4**. The solid lines are best fits to quadratic functions $F(n) = a + bn + cn^2$, demonstrating that these parameters follow quadratic decays with n. Best-fit parameters: $a = 3.8793$, $b = 0.0414$ and $c = -0.0034$ with $R^2 = 0.9921$; $a = 2.7148$, $b = -0.0061$ and $c = -0.0007$ with $R^2 = 0.9923$; $a = 2.6429$, $b = -0.0038$ and $c = -0.0005$ with $R^2 = 0.9946$, for $d_{(Ln\cdots Ln)}$, $d_{(O\cdots O)}$ and $\bar{x}_{(Ln-X)}$, respectively.

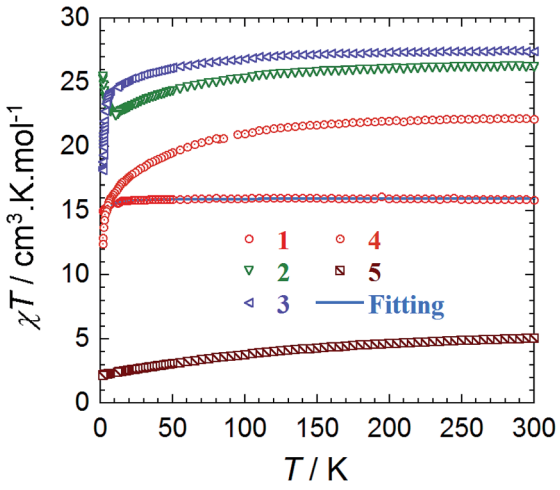

Fig. 3 Temperature dependence of the magnetic susceptibility χT at 1000 Oe for complexes **1–5**. For complex **1**, the best-fit parameters (solid blue line) obtained for the χT curve are $J = -0.01$ cm^{-1} and $g = 2.01$.

shows that the magnetization rapidly increases with applied dc field to approach magnetic saturation above 7 T, at which a value of 14 μ_B is reached (Fig. S3†). This true saturation reveals the absence of magnetic anisotropy within this complex. The superimposition of the *M vs.* HT^{-1} data on a single master curve further confirms this result, which is expected for isotropic systems such as Gd^{III}. Direct current magnetic susceptibility studies for complexes **2–5** were also carried out, and can also be seen in Fig. 3. The room temperature χT values of 26.19 (**2**), 27.39 (**3**), 22.11 (**4**) and 5.03 (**5**) cm^3 K mol^{-1} are close to the expected values for two uncoupled lanthanide ions: Dy^{III} ($^6H_{15/2}$, $S = 5/2$, $\chi T = 28.34$ cm^3 K mol^{-1}), Ho^{III} ($^5I_8$, $S = 2$, $\chi T = 28.14$ cm^3 K mol^{-1}), Er^{III} ($^4I_{13/2}$, $S = 5/2$, $\chi T = 22.96$ cm^3 K mol^{-1}), and Yb^{III} ($^2F_{7/2}$, $S = 1/2$, $\chi T = 5.12$ cm^3 K mol^{-1}).

For the Dy^{III} analogue, **2**, as the temperature decreases, the χT product decreases gradually until reaching a minimum value of 22.41 cm^3 K mol^{-1} at 11 K, followed by a sharp increase to a maximum value of 25.46 cm^3 K mol^{-1} at 1.8 K. The decrease is most likely caused by the depopulation of the Stark sublevels and/or significant magnetic anisotropy, while the latter increase can be attributed to weak ferromagnetic interactions between the Dy^{III} ions. The origin of this interaction will be discussed further in the following section from the perspective of the performed *ab initio* calculations. In systems **3–5**, upon lowering the temperature, the χT product decreases continuously until reaching a minimum value at 1.8 K. These results may point towards weak antiferromagnetic intramolecular interactions and/or thermal depopulation of the Stark sublevels. The field dependent magnetization data for complexes **2–5** are shown in the ESI (Fig. S4†), plotted as *M vs. H* and *M vs.* HT^{-1}. The resulting magnetization curves do not saturate (*M vs. H*), nor superimpose on a single master curve (*M vs.* HT^{-1}), thus indicating the presence of significant anisotropy and/or low-lying excited states present in all complexes.

To probe potential slow magnetic relaxation, ac susceptibility measurements were carried out for complexes **2–5**. The Ho^{III} analogue did not exhibit an out-of-phase signal under the measurement conditions, hence it does not behave as a SMM. For complex **2**, significant quantum tunnelling of the magnetization (QTM)[30] was observed under zero applied dc field, evident from the lack of clear full peaks. In order to minimize the QTM, ac susceptibility measurements were performed under an optimal applied dc field of 1800 Oe in the temperature range of 1.8–7.5 K (Fig. 4).

The presence of peaks shifting to lower frequency with decreasing temperatures for the out-of-phase (χ'') susceptibility, indicates potential SMM behaviour. However, by fitting the magnetic data between 1.8 and 3.5 K with the Arrhenius equation ($\tau = \tau_0 \exp(U_{eff}/kT)$), a barrier of 3.3 K was obtained with a pre-exponential factor (τ_0) of 0.04336 s, suggesting that the QTM may be too efficient in this system, such that the height of the barrier is compromised. In order to acquire more insight into the electronic structure of the magnetic sites, *ab initio* calculations[31] were performed on **2**. CASSCF/RASSI/SINGLE_ANISO calculations[31,32] were completed on the individual Dy^{III} sites, keeping the entire molecule "as is", with only the computational substitution of one of the Dy^{III} sites by the diamagnetic Lu^{III}. Results of the *ab initio* calculations can be seen in Table S3.† In particular, the large values of the g_x and g_y components of the g tensor in the ground Kramers doublet of individual Dy^{III} ions are in line with the observed fast tunnelling of magnetization in **2**. As was previously stated,[17] the large values of the perpendicular components (x, y) in the ground state interact with the magnetic field present in the crystal and induce tunnelling of the magnetization. The obtained values for **2** are at least two orders of magnitude larger than in current well-performing molecular magnets.[29,33] The upturn of the magnetic susceptibility curve upon lowering of temperature is indicative of weak ferromagnetic coupling at low temperature. The nature of this interaction is mainly dipolar, given the small angle (~12.2°) between the main anisotropy axes on Dy^{III} sites and the Dy–Dy axis, thus favouring the stabilization of the ferromagnetic arrangement of the local moments (Fig. 5). As for the Er^{III} compound, **4**, frequency dependent signal (Fig. S5†) is clearly observed under an applied dc field of 1200 Oe, thus indicating its SMM nature. An effective barrier of 21 K ($\tau_0 = 2.75 \times 10^{-6}$ s) was calculated by fitting the magnetic data *via* the

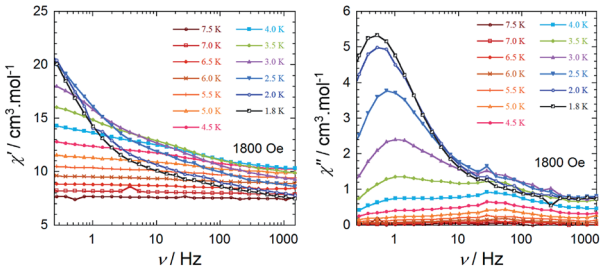

Fig. 4 Frequency (ν) dependence of the in-phase (χ', left) and out-of-phase (χ'', right) magnetic susceptibility at the indicated temperatures for **2** under an applied optimum dc field of 1800 Oe.

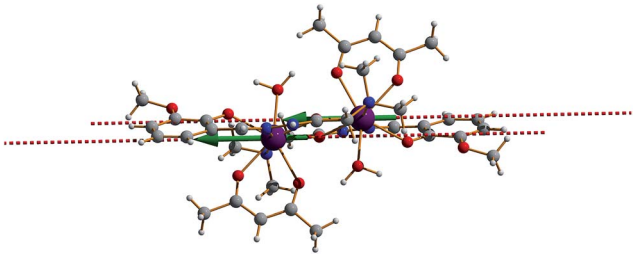

Fig. 5 Orientations of the anisotropy axes (dashed line) in **2**. Colour scheme: Dy-purple, O-red, C-grey, N-blue, H-white. Green arrows represent the orientation of the local magnetic moments on Dy^{III} sites in the coupled ground state, arrangement driven by ferromagnetic dipolar coupling.

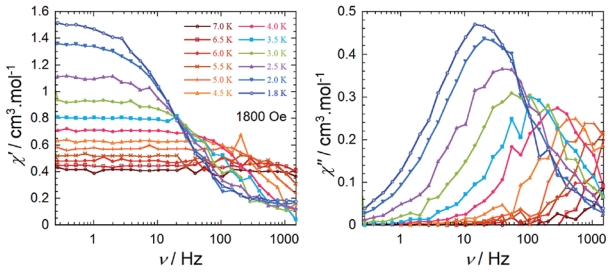

Fig. 6 Frequency (ν) dependence of the in-phase (χ′, left) and out-of-phase (χ″, right) magnetic susceptibility at the indicated temperatures for **5** under an applied optimum dc field of 1800 Oe.

Arrhenius equation (Fig. S5†). The observed overlapping of peaks at low frequency is attributed to the presence of QTM.

The frequency scan of the ac susceptibility in zero dc field performed at 2 K for the Yb^{III} analogue, **5**, reveals the absence of any growing out-of-phase signal. However, the application of an external dc field of 1800 Oe successfully shifts the characteristic maximum of χ'' values to lower frequencies where full peaks may be observed (Fig. 6). The relaxation time was extracted from the fit of the frequency dependence of the ac susceptibility data between 1.8 and 7 K.

The temperature dependence of the relaxation time follows the Arrhenius law between 3.5 and 5.5 K with an energy barrier $U_{eff} = 22$ K and $\tau_0 = 2.13 \times 10^{-6}$ s (Fig. S6†). Below 3.5 K, the relaxation time deviates from a thermally activated process possibly due to a direct process allowed in a low symmetry environment.[34] Furthermore, the distribution of the relaxation time, α, does not exceed 0.3 at lower-temperature and is close to zero up to 5 K.[35]

Conclusions

In summary, a series of centrosymmetric dinuclear complexes have been synthesized and studied for their structural and magnetic properties; in particular as relates to the effects of lanthanide contraction and anisotropy of metal ions. The highly-flexible multidentate ligand H_2ovgrd allowed for similar structural arrangements, with subtle changes, through Gd^{III} to Yb^{III} as the radius of the metal ions decreased. The shielding constants for 4f electrons in each complex were calculated and compared with the ionic radii, confirming the presence of significant lanthanide contraction within these systems. By probing the magnetic properties, the gadolinium analogue, **1**, reveals a weak antiferromagnetic intramolecular interaction, with $J = -0.01$ cm^{-1} and $g = 2.01$. The Dy analogue (**2**) did not exhibit SMM properties, which has been revealed by *ab initio* calculations to be due to the larger values of g_x and g_y in the ground doublet of individual Dy^{III} ions, as well as the weak magnetic interaction between Dy^{III} sites, mainly driven by ferromagnetic dipolar interaction. However, the Er^{III} (**4**) and Yb ^{III} (**5**) counterparts were found to exhibit slow relaxation of the magnetization under an applied dc field. This new family of Ln_2 compounds reveal a further glimpse into the uniqueness of the lanthanide series, through the study of the changes in physical properties while retaining their structural similitudes.

Acknowledgements

We gratefully acknowledge financial support towards this work from NSERC, CFI grants Canada. L. U. is a postdoc of the FWO-Vlaanderen.

Notes and references

1 R. Layfield and M. Murugesu, *Lanthanides and Actinides in Molecular Magnetism*, John Wiley & Sons, 2015.
2 D. N. Woodruff, R. E. P. Winpenny and R. A. Layfield, *Chem. Rev.*, 2013, **113**, 5110–5148.
3 F. Habib and M. Murugesu, *Chem. Soc. Rev.*, 2013, **42**, 3278–3288.
4 L. Sorace, C. Benelli and D. Gatteschi, *Chem. Soc. Rev.*, 2011, **40**, 3092.
5 J. J. L. Roy, I. Korobkov, J. E. Kim, E. J. Schelter and M. Murugesu, *Dalton Trans.*, 2014, **43**, 2737–2740.
6 J. J. Le Roy, S. I. Gorelsky, I. Korobkov and M. Murugesu, *Organometallics*, 2015, **34**, 1415–1418.
7 S. Hino, M. Maeda, K. Yamashita, Y. Kataoka, M. Nakano, T. Yamamura, H. Nojiri, M. Kofu, O. Yamamuro and T. Kajiwara, *Dalton Trans.*, 2013, **42**, 2683.
8 J. D. Rinehart and J. R. Long, *Dalton Trans.*, 2012, **41**, 13572–13574.
9 A. Watanabe, A. Yamashita, M. Nakano, T. Yamamura and T. Kajiwara, *Chem.–Eur. J.*, 2011, **17**, 7428–7432.
10 J. D. Rinehart, M. Fang, W. J. Evans and J. R. Long, *J. Am. Chem. Soc.*, 2011, **133**, 14236–14239.
11 C. R. Ganivet, B. Ballesteros, G. de la Torre, J. M. Clemente-Juan, E. Coronado and T. Torres, *Chem.–Eur. J.*, 2013, **19**, 1457–1465.
12 J. J. L. Roy, I. Korobkov and M. Murugesu, *Chem. Commun.*, 2014, **50**, 1602–1604.
13 J. J. Le Roy, L. Ungur, I. Korobkov, L. F. Chibotaru and M. Murugesu, *J. Am. Chem. Soc.*, 2014, **136**, 8003–8010.
14 K. R. Meihaus and J. R. Long, *J. Am. Chem. Soc.*, 2013, **135**, 17952–17957.
15 N. F. Chilton, *Inorg. Chem.*, 2015, **54**, 2097–2099.

16 R. J. Blagg, L. Ungur, F. Tuna, J. Speak, P. Comar, D. Collison, W. Wernsdorfer, E. J. L. McInnes, L. F. Chibotaru and R. E. P. Winpenny, *Nat. Chem.*, 2013, **5**, 673–678.
17 L. Ungur and L. F. Chibotaru, *Phys. Chem. Chem. Phys.*, 2011, **13**, 20086–20090.
18 J. D. Rinehart, M. Fang, W. J. Evans and J. R. Long, *Nat. Chem.*, 2011, **3**, 538–542.
19 F. Habib, P.-H. Lin, J. Long, I. Korobkov, W. Wernsdorfer and M. Murugesu, *J. Am. Chem. Soc.*, 2011, **133**, 8830–8833.
20 F. Habib, G. Brunet, V. Vieru, I. Korobkov, L. F. Chibotaru and M. Murugesu, *J. Am. Chem. Soc.*, 2013, **135**, 13242–13245.
21 G.-F. Xu, Q.-L. Wang, P. Gamez, Y. Ma, R. Clérac, J. Tang, S.-P. Yan, P. Cheng and D.-Z. Liao, *Chem. Commun.*, 2010, **46**, 1506–1508.
22 X. Yi, K. Bernot, F. Pointillart, G. Poneti, G. Calvez, C. Daiguebonne, O. Guillou and R. Sessoli, *Chem.–Eur. J.*, 2012, **18**, 11379–11387.
23 F. Pointillart, Y. Le Gal, S. Golhen, O. Cador and L. Ouahab, *Chem.–Eur. J.*, 2011, **17**, 10397–10404.
24 K. Suzuki, R. Sato and N. Mizuno, *Chem. Sci.*, 2013, **4**, 596–600.
25 P. H. Lin, T. J. Burchell, R. Clerac and M. Murugesu, *Angew. Chem., Int. Ed.*, 2008, **47**, 8848.
26 A. J. Hutchings, F. Habib, R. J. Holmberg, I. Korobkov and M. Murugesu, *Inorg. Chem.*, 2014, **53**, 2102–2112.
27 D. Aguilà, L. A. Barrios, V. Velasco, L. Arnedo, N. Aliaga-Alcalde, M. Menelaou, S. J. Teat, O. Roubeau, F. Luis and G. Aromí, *Chem.–Eur. J.*, 2013, **19**, 5881–5891.
28 E. A. Quadrelli, *Inorg. Chem.*, 2002, **41**, 167–169.
29 L. Ungur, J. J. Le Roy, I. Korobkov, M. Murugesu and L. F. Chibotaru, *Angew. Chem., Int. Ed.*, 2014, **53**, 4413–4417.
30 L. Thomas, F. Lionti, R. Ballou, D. Gatteschi, R. Sessoli and B. Barabara, *Nature*, 1996, **383**, 145–147.
31 F. Aquilante, V. L. De, N. Ferré, G. Ghigo, P. A. Malmgvist, P. Neogrády, T. B. Pedersen, M. Pitonák, M. Reiher, B. O. Roos, L. Serrano-Andrés, M. Urban, V. Veryazov and R. Lindh, *J. Comput. Chem.*, 2010, **31**, 224–247.
32 L. F. Chibotaru and L. Ungur, *J. Chem. Phys.*, 2012, **137**, 064112.
33 Y.-N. Guo, G.-F. Xu, W. Wernsdorfer, L. Ungur, Y. Guo, J. Tang, H.-J. Zhang, L. F. Chibotaru and A. K. Powell, *J. Am. Chem. Soc.*, 2011, **133**, 11948–11951.
34 F. Pointillart, B. Le Guennic, S. Golhen, O. Cador, O. Maury and L. Ouahab, *Chem. Commun.*, 2013, **49**, 615–617.
35 K. S. Cole and R. H. Cole, *J. Chem. Phys.*, 1941, **9**, 341–352.